The Effect of Suspended Particulate Matter on the Performance of High Frequency Sonars in Turbid Coastal Waters

S.D. Richards [1], A.D. Heathershaw [1], N.R. Brown [2] & T.G. Leighton [2]

(1) Defence Evaluation & Research Agency,
DERA Winfrith,
Winfrith Technology Centre, Dorset DT2 8XJ, United Kingdom
E-mail: sdrichards@dra.hmg.gb

(2) Institute of Sound & Vibration Research,
University of Southampton,
Highfield, Southampton S017 1BJ, United Kingdom

Abstract

Shallow coastal environments are characterised by high levels of suspended mineral particles relative to the open ocean and such suspensions can have a significant effect on the performance of high frequency sonars operating in these environments through thermo-viscous absorption and scattering. This paper shows how the increased attenuation due to these processes can be calculated and results presented demonstrate that such calculations should be included in future high frequency, shallow water, sonar performance models.

1. Introduction

Classically, efforts in sonar performance prediction modelling have concentrated on the low frequency, long range, anti-submarine warfare (ASW) scenarios in the deep ocean (so-called 'blue-water'), well away from coastal influences. Sonar applications in shallow, coastal waters employ relatively high frequencies, in the range 50 - 300 kHz, and operate over shorter ranges, of the order several hundred metres. Shallow coastal environments are characterised by high concentrations of suspended mineral particles relative to the open ocean, resulting from the action of rivers discharging into the sea or from the actions of waves and tidal currents stirring up bottom sediments. Previous calculations [1, 2] have shown that such suspensions can lead to significant additional acoustic attenuation at high frequencies for quite moderate concentrations of order 0.1 kg m^{-3}. Concentrations of this level have been detected several tens of kilometres offshore in sediment plumes (e.g. South Atlantic offshore of the Amazon river [3], the Yellow Sea and the East China Sea offshore of the Yellow and Yangtze rivers [4]), and may easily be an order of magnitude greater in some river estuaries and in the beach surf zone.

2. Attenuation theory

Sound attenuation in seawater containing suspended particulate matter may be considered to be the sum of attenuation due to the clear seawater and the additional attenuation due to the suspended particles. Existing sonar performance models consider only the attenuation in clear seawater, neglecting the effects of the particles.

The sound intensity attenuation coefficient α is defined by the expression

$$I = I_0 e^{-2\alpha r} \tag{1}$$

where I_0 is the initial sound intensity and I is the intensity after propagation over range r. In this equation α is in units of Nepers m^{-1}, but units of dB m^{-1} have been used in the rest of this paper to be consistent with units used in sonar work.

The attenuation coefficient in seawater containing suspended solid particles may be written

$$\alpha = \alpha_w + \alpha_v + \alpha_s \tag{2}$$

where α_w, α_v and α_s are the attenuation coefficients due to clear seawater, viscous absorption by suspended particles and scattering by suspended particles respectively. Simple expressions for the attenuation coefficients due to viscous absorption and scattering have been used in this work, and these are discussed below. These simple models have been validated by comparison with a more complete numerical model of the physical processes involved [5].

2.1. Attenuation in clear seawater

The absorption in clear seawater may be considered as the sum of absorption due to pure water, through volume and shear viscosity, and absorption due to two ionic relaxation mechanisms involving magnesium sulphate and boric acid. Absorption due to ionic relaxations involving other salts is negligible.

Several empirically derived expressions exist in the literature for calculating the acoustic attenuation coefficient of seawater (e.g. [6, 7, 8, 9, 10]). The one that appears to be the most complete for use at high frequencies is that of Francois & Garrison [9, 10], and it is their expression that has been used in this work.

2.2. Viscous absorption

Viscous absorption arises as a result of the density difference between the fluid and the solid particles. Since the particles are generally more dense than the fluid they have more inertia than an equivalent volume of fluid. This causes the oscillatory motion of the particles resulting from the incident sound field to lag behind that of the fluid, and there will therefore be a boundary layer in the fluid at the surface of each particle in which there is a velocity gradient. Since the fluid has a finite viscosity, this velocity gradient leads to frictional heat generation and hence loss of energy from the sound field.

Urick [11] derived an expression for the viscous absorption attenuation coefficient for spherical particles based on consideration of the expression for viscous drag developed by Stokes [12]. Urick's expression can be written

$$\alpha_v = (10 \log e^2) \left(\frac{\epsilon k (\sigma - 1)^2}{2} \left[\frac{s}{s^2 + (\sigma + \delta)^2} \right] \right) \quad \text{dB m}^{-1} \tag{3}$$

with

$$\delta = \frac{1}{2} \left[1 + \frac{9}{2\beta a} \right] \quad , \quad s = \frac{9}{4\beta a} \left[1 + \frac{1}{\beta a} \right] \tag{4}$$

where ϵ is the volume fraction of suspended material, $k = \omega/c$ is the wavenumber of the incident compression waves with c the compression wave speed, $\sigma = \rho'/\rho$ is the ratio of the solid density to the fluid density, a is the particle radius and $\beta = \sqrt{\omega/2\nu}$ is the reciprocal of the skin depth for viscous shear waves, with ω the angular frequency and ν the kinematic viscosity of the fluid.

2.3. Scattering

Many workers have investigated sound scattering from suspended spheres, and expressions may easily be found in the literature (e.g. [13]) for the far-field scattering form function, f_∞. Such approaches generally treat the particle as a homogeneous sphere which may be: rigid and movable; rigid and immovable; or elastic. The elastic models in particular lead to complicated scattering form functions owing to resonant excitation. However, when dealing with naturally occurring sediment populations, the particles will be irregular in shape and size, and each particle will have differences in the detailed structure of the scattering form functions. Therefore, when considering the combined effect of a large number of such irregular particles, such details become smeared out, and it is appropriate to use a simpler form for the scattering form function. Such an approach was used by Johnson [14] in developing

the so called high-pass model for backscattered intensity from a fluid sphere. Here, a simple polynomial in $x = ka$ is used to represent the scattering form function approximately by requiring that it fits the form of f_∞ exactly in the Rayleigh (small x) and geometric (large x) regimes. The exact amplitude scattering form function for a sphere varies as x^2 in the Rayleigh regime and becomes constant in the geometric regime, so a polynomial fit to this resembles the response curve of a high-pass filter, hence the nomenclature.

Sheng and Hay [15] constructed a high-pass model for the attenuation coefficient for scattering by a suspension of spheres, and their expression may be written

$$\alpha_s = (10\log e^2)\frac{\epsilon K_\alpha x^4}{a\left(1 + \xi x^2 + \frac{4}{3}K_\alpha x^4\right)} \quad \text{dB m}^{-1} \tag{5}$$

where

$$K_\alpha = \frac{1}{6}\left(\gamma_\kappa^2 + \frac{\gamma_\rho^2}{3}\right) \tag{6}$$

and ξ is an adjustable constant ≥ 1. The ξ term allows the form of the polynomial to be adjusted to improve the fit to experimental data for intermediate x values. The terms γ_κ and γ_ρ are the compressibility and density contrasts given by

$$\gamma_\kappa = \frac{\kappa' - \kappa}{\kappa} \tag{7}$$

$$\gamma_\rho = \frac{3(\rho' - \rho)}{2\rho' + \rho} \tag{8}$$

where κ and κ' are the bulk compressibilities of the fluid and solid respectively.

3. Sonar performance calculations

In this paper simple sonar equation calculations have been used to investigate the effect of suspended particulate matter on sonar performance. These calculations, which are based on References [16, 17], assume isovelocity conditions and uniform bathymetry, and multiple propagation paths have been neglected.

The active sonar equation for signal excess (SE) may be written

$$SE = EL - BG + PG \tag{9}$$

where EL is the target echo level, BG is the combined noise and reverberation background and PG is the processor gain.

The target echo level may be written

$$EL = SL + TS - 2TL + V_{pt} \tag{10}$$

where SL is the source level, TS is the target strength, TL is the one-way transmission-loss and V_{pt} is a vertical beam pattern correction factor to allow for target echoes which arrive off the main beam axis.

The transmission loss is assumed to be identical for both the forward and reflected pulse, and is approximated here by the sum of spherical spreading and volume attenuation

$$TL = 20\log(r) + \alpha r \tag{11}$$

where r is the one-way distance to the target and α is the total attenuation coefficient for seawater containing suspended particles, given by Equation 2.

The combined background level, BG is given by

$$BG = 10 \log \left[10^{RL_s/10} + 10^{RL_b/10} + 10^{RL_v/10} + 10^{NL/10} \right] \tag{12}$$

where RL_s, RL_b, RL_v are the surface, bottom and reverberation levels and NL is the noise level.

The surface and bottom reverberation levels are given by

$$RL_s = SL - 2TL + \Phi + 10 \log \left(\frac{rc\tau}{2} \right) + S_s + V_s \tag{13}$$

$$RL_s = SL - 2TL + \Phi + 10 \log \left(\frac{rc\tau}{2} \right) + S_b + V_b \tag{14}$$

where Φ is the equivalent beamwidth for sea surface and seabed reverberation, c is the sound speed, τ is the pulse length, S_s and S_b are the surface and bottom scattering strengths and V_s and V_b are vertical beam pattern corrections for surface and bottom scattering.

Calculation of the equivalent beamwidth Φ uses an approximation employed in the Searay model [18]. Similarly, the surface scattering strength and bottom scattering strength use the same methods as the Searay model. The quantity S_s is expressed as a function of grazing angle, frequency and wind speed, and S_b is expressed as a function of grazing angle, frequency and bottom type, m, where m can take any value between 1 (mud) and 4 (rock).

The volume reverberation level is given by

$$RL_v = SL - 2TL + \Psi + 20 \log(r) + 10 \log \left(\frac{c\tau}{2} \right) + S_v \tag{15}$$

where Ψ is the equivalent beamwidth for volume reverberation and S_v is the volume scattering strength. In this paper the volume scattering strength is simply taken to be [16]

$$S_v = -88.6 + 7 \log(f(\text{kHz})) \tag{16}$$

It is realised that the presence of suspended particulate matter that is being considered in this paper will influence the volume scattering strength. The model for volume scattering strength should therefore be modified to take this into account, and this will be done in future investigations.

The ambient noise level at the receiver is given by

$$NL = Ns + 10 \log(B) - DI \tag{17}$$

where Ns is the noise spectrum level, B is the bandwidth of the receiver system and DI is the directivity index of the receive array.

In this paper we have used the Searay approximation for the directivity index of a rectangular array, together with the expression for the noise spectrum used in the Searay model.

The processor gain, PG, is given by

$$PG = 10 \log(B\tau) \tag{18}$$

4. Laboratory measurements

A series of laboratory experiments to investigate viscous absorption by aqueous suspensions of mineral particles is being undertaken by Brown & Leighton at the Institute of Sound and Vibration Research, University of Southampton, United Kingdom [19, 20]. These experiments are described in a separate paper at this conference [21]. Preliminary experimental data presented in that paper shows a general increase in attenuation with increasing frequency in agreement with theoretical predictions. The measured attenuation is, however, greater than predicted. The reasons for this are not yet clear but it is possible that the additional attenuation results from effects not included in the theory, such as turbulence. This will be investigated further.
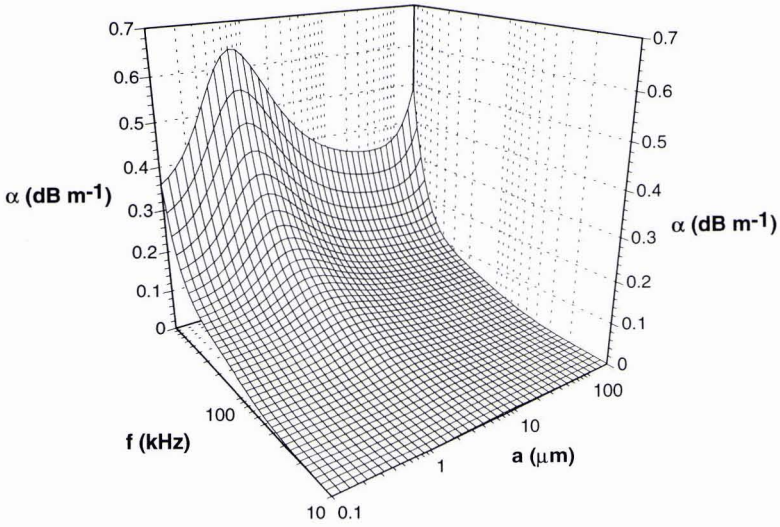
Figure 1: Absorption coefficient for seawater containing 0.2 kg m^{-3} suspended quartz particles as a function of frequency and particle radius

5. Results

Figure 1 shows the total attenuation coefficient due to absorption by clear seawater and viscous absorption and scattering by a suspension of quartz particles of concentration 0.2 kg m^{-3}, as a function of frequency and particle radius, calculated using Equations (3) and (5). This figure clearly demonstrates how the viscous absorption peaks at a particular particle size for a given frequency. The attenuation also increases as the frequency and particle size become large (i.e. increasing ka) due to scattering. The attenuation due to the particles is added to the background attenuation due to the clear seawater in this figure, calculated using the Francois & Garrison expression for a temperature of 15°C and a salinity of 35 on the Practical Salinity Scale.
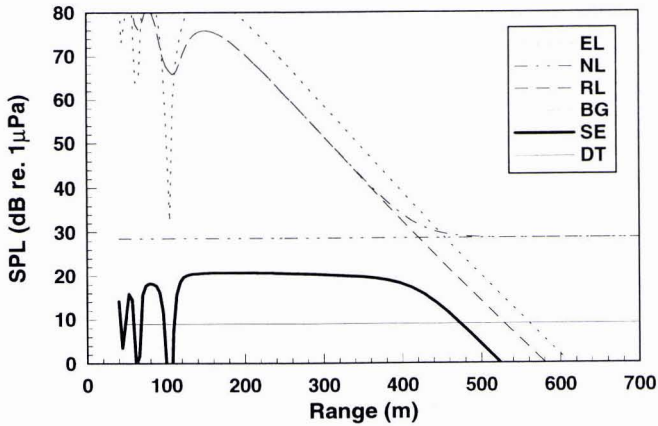

Figure 2: Sound Pressure Level as a function of range for various terms in the sonar equation model (see text)

Figure 2 shows the results of the sonar equation model, using some typical sonar parameters for a sonar operating at 120 kHz in shallow water. In this calculation a suspension of quartz particles of radius 1 μm with a concentration of 0.2 kg m^{-3} was used in the calculation of the absorption coefficient, together with the attenuation due to clear seawater using the Francois & Garrison expression for a temperature of 15°C, a salinity of 35 on the Practical Salinity Scale and a pressure corresponding that at half the water depth of 40 m. The target strength was taken to be -25 dB, the target depth was 40 m (i.e. at the seabed), the array depth was 20 m, and the detection threshold was 9 dB re. 1 μPa. The reverberation level (RL) shown in the figure is the total reverberation level due to seabed, surface and volume reverberation, using a wind speed of 15 knots and a bottom type of 2 (sand).

The detection range may be defined as the range within which the signal excess exceeds the detection threshold, giving a detection range of around 473 m in Figure 2. This may be compared with a detection range of about 660 m in the absence of the particles, as shown in Figure 3, which shows the signal excess with and without the 0.2 kg m^{-3} suspension of 1 μm quartz particles
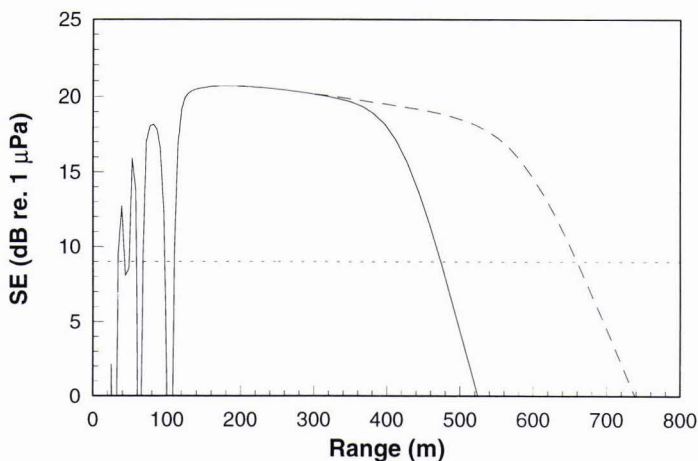

Figure 3: Signal excess with (solid) and without (dashed) 0.2 kg m^{-3} suspension of 1 μm quartz particles. The dotted line shows the detection threshold, DT

Figure 4 shows the variation in detection range with concentration of suspended particles for three different particle sizes, at a frequency of 120 kHz. This shows that there is a significant reduction in detection range for all particle sizes at even quite moderate concentrations of suspended particles. The greatest reduction in detection range at this frequency occurs for $a = 3$ μm, with smaller, but still significant, reduction for the other particle sizes. This is to be expected, as Figure 1 shows that the viscous absorption peak occurs for particle sizes of around 3 μm for a frequency of 120 kHz.

6. Conclusions

This paper has shown how the additional acoustic attenuation at high frequencies due to viscous absorption and scattering by suspended mineral particles in turbid seawater may be taken into account in sonar performance models by using a modified absorption coefficient. This approach has been used to incorporate the effects into a simple, isovelocity, single path, sonar equation model with uniform bathymetry and the results presented demonstrate that concentrations in the range commonly found in shallow coastal waters can have a significant impact on the detection range of high frequency sonar systems. It is therefore recommended that future predictive models of the performance of high frequency sonars in turbid coastal waters should take the additional attenuation due to the suspended particles into account. This would require accurate knowledge of the suspended particle populations, which might come from *in-situ* measurements or remote sensing and assimilation into hydrodynamic models. The latter would be important for Rapid Environmental Assessment (REA).
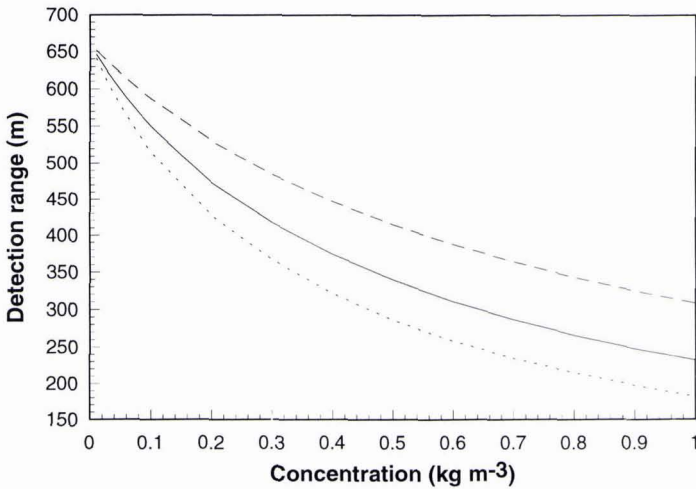
Figure 4: Detection range as a function of concentration for $a = 1\,\mu\mathrm{m}$ (solid), $a = 3\,\mu\mathrm{m}$ (dotted), $a = 10\,\mu\mathrm{m}$ (dashed)

7. Acknowledgements

References

[1] A D Heathershaw, S D Richards & P D Thorne, (1996), 'Acoustic absorption and scattering by suspended sediments in turbid coastal waters', (unpublished)

[2] S D Richards, A D Heathershaw & P D Thorne, (1996), 'The effect of suspended particulate matter on sound attenuation in seawater', *J. Acoust. Soc. Am.*, **100**, 1447-1450

[3] C A Nittrouer & D J DeMaster (Ed.), (1986), 'Sedimentary processes on the Amazon continental shelf', *Cont. Shelf Res.*, **6**, 1–357

[4] J D Milliman & J Qingming (Ed.), (1985), 'Sediment dynamics of the Changjiang Estuary and the adjacent East China Sea', *Cont. Shelf Res.*, **4**, 1–251

[5] S D Richards & A D Heathershaw, (1996), 'An investigation of viscous absorption of sound energy in turbid seawater at mine-hunting frequencies', DRA Report (unpublished), March 1996

[6] W H Thorpe, (1965), 'Deep ocean sound attenuation in the sub and low kilocyle per second range', *J. Acoust. Soc. Am.*, **42**, 648–654

[7] M Schulkin & H W Marsh, (1962), 'Sound absorption in seawater', *J. Acoust. Soc. Am.*, **34**, 864–865

[8] F H Fisher & V P Simmons, (1977), 'Sound absorption in sea water', *J. Acoust. Soc. Am.*, **92**, 558–564

[9] R E Francois & G R Garrison, (1982), 'Sound absorption based on ocean measurements: Part I: Pure water and magnesium sulfate contributions', *J. Acoust. Soc. Am.*, **72**, 896–907

[10] R E Francois & G R Garrison, (1982), 'Sound absorption based on ocean measurements: Part II: Boric acid contribution and equation for total absorption', *J. Acoust. Soc. Am.*, **72**, 1879–1890

[11] R J Urick, (1948), 'The absorption of sound in suspensions of irregular particles', *J. Acoust. Soc. Am.*, **20**, 283–289

[12] G G Stokes, (1922), 'On the effect of internal friction of fluids on the motion of pendulums', *Math. and Phys. Papers*, **3**, 1–122

[13] Faran, Jr., J J, (1951), 'Sound scattering by solid cylinders and spheres', *J. Acoust. Soc. Am.*, **23**, 405–418

[14] R K Johnson, (1977), 'Sound scattering from a fluid sphere revisited', *J. Acoust. Soc. Am.*, **61**, 375–377

[15] J Sheng & A E Hay, (1988), 'An examination of the spherical scatterer approximation in aqueous suspensions of sand', *J. Acoust. Soc. Am.*, **83**, 598–610

[16] P A G Thomson & I Foster, (1994), 'Sensitivity study and review of current minehunting sonar performance prediction modelling', DRA Report (unpublished), October 1994

[17] P A G Thomson, (1997), Private communication

[18] S M Tuovila, (1989), 'Searay Sonar Simulation Model', NCSC TN 946-88

[19] N R Brown & T G Leighton, (1996), 'Sound Absorption by Suspended Particulate Matter,' ISVR Contract Report No. 96/22

[20] N R Brown & T G Leighton, (1997), 'Sound Absorption by Suspended Particulate Matter,' ISVR Contract Report No. 97/04

[21] N R Brown, T G Leighton, S D Richards & A D Heathershaw, (1997), 'Sound absorption by suspended particulate matter', this conference.